

# Novel copper redox-based cathode materials for room-temperature sodium-ion batteries\*

Xu Shu-Yin(徐淑银), Wu Xiao-Yan(吴晓燕), Li Yun-Ming(李云明),  
Hu Yong-Sheng(胡勇胜)<sup>†</sup>, and Chen Li-Quan(陈立泉)

Beijing National Laboratory for Condensed Matter Physics, Institute of Physics,  
Chinese Academy of Sciences, Beijing 100190, China

(Received 22 September 2014; published online 29 September 2014)

Layered oxides of P2-type  $\text{Na}_{0.68}\text{Cu}_{0.34}\text{Mn}_{0.66}\text{O}_2$ , P2-type  $\text{Na}_{0.68}\text{Cu}_{0.34}\text{Mn}_{0.50}\text{Ti}_{0.16}\text{O}_2$ , and O'3-type  $\text{NaCu}_{0.67}\text{Sb}_{0.33}\text{O}_2$  were synthesized and evaluated as cathode materials for room-temperature sodium-ion batteries. The first two materials can deliver a capacity of around 70 mAh/g. The  $\text{Cu}^{2+}$  is oxidized to  $\text{Cu}^{3+}$  during charging, and the  $\text{Cu}^{3+}$  goes back to  $\text{Cu}^{2+}$  upon discharging. This is the first demonstration of the highly reversible change of the redox couple of  $\text{Cu}^{2+}/\text{Cu}^{3+}$  with high storage potential in secondary batteries.

**Keywords:** energy storage, sodium-ion battery, cathode, copper redox

**PACS:** 82.45.Yz, 82.47.Aa, 82.47.Cb, 84.60.-h

**DOI:** 10.1088/1674-1056/23/11/118202

## 1. Introduction

Lithium-ion batteries are widely used in portable electronic devices and would be the best choice for electric vehicles. However, the rarity and non-uniform distribution of lithium in the Earth's crust may limit their large scale application in renewable energy.<sup>[1-3]</sup> In this regard, room-temperature sodium-ion batteries have again attracted great interest recently.<sup>[4,5]</sup> Sodium has physical and chemical properties similar to those of lithium, while there is no limitation of sodium resources. This could pave the way for sodium-ion batteries' large-scale application in renewable energy and smart grids.<sup>[6,7]</sup>

Until now, many electrode materials including anodes and cathodes have been proposed.<sup>[8-21]</sup> In particular, layered oxides with a general formula of  $\text{Na}_x\text{MO}_2$  ( $M = \text{Ni}, \text{Co}, \text{Mn}, \text{Fe}, \text{Cr}, \text{etc.}$ ) have been widely investigated in the last few years.<sup>[8-10,22-26]</sup> In general, the compounds tend to form a P2-type structure if  $x \leq 0.8$  except when there are some special dopings like Li into the transition metal layer;<sup>[27-30]</sup> when  $x > 0.8$ , the materials tend to form an O3-type structure. Note that the notations of P2 and O3 were defined by Delmas *et al.*<sup>[31]</sup> They represent different ways of the stacking of the oxygen layer and coordination environment of the alkali ions. Higher reversible capacity can be obtained for O3-type compounds, but with low stability.<sup>[22,25,26]</sup> The P2 phase materials seem to deliver better cycle performance and rate capability in sodium-ion batteries.<sup>[30,32]</sup> The trigonal prismatic site occupied by the  $\text{Na}^+$  ion in P2 phase is larger than the corre-

sponding octahedral site in O3 phase; thus  $\text{Na}^+$  ion transport in P2 phase is easier and faster. Layered electrode materials based on Ni or Co element show excellent performance in terms of high storage capacity, rate capability, and cycling stability.<sup>[8,24,26,27,30]</sup> However, Ni and Co are toxic and their oxides are relatively expensive, which would certainly increase the cost of the battery and is unfavorable for large-scale energy storage applications.

Taking into account the low cost and environmental friendliness of Cu, copper based electrode materials are very attractive. However, the highly reversible transfer between  $\text{Cu}^{2+}$  and  $\text{Cu}^{3+}$  in electrode materials is hard to realize in secondary batteries. In the present work, we design and prepare three different layered electrode materials based on copper: P2-type  $\text{Na}_{0.68}\text{Cu}_{0.34}\text{Mn}_{0.66}\text{O}_2$ , P2-type  $\text{Na}_{0.68}\text{Cu}_{0.34}\text{Mn}_{0.50}\text{Ti}_{0.16}\text{O}_2$ , and O3'-type  $\text{NaCu}_{0.67}\text{Sb}_{0.33}\text{O}_2$ . Surprisingly, the three materials all show reversible Na extraction and insertion with small polarization, which could be due to the reversible change of  $\text{Cu}^{2+}/\text{Cu}^{3+}$  redox couple, because the valences of Mn and Ti are already 4+ in the starting materials, i.e., impossible to oxidize upon Na extraction. The first two materials can deliver a capacity of around 70 mAh/g. To the best of our knowledge, this is the first time to realize the reversible change of  $\text{Cu}^{2+}/\text{Cu}^{3+}$  redox couple with small polarization. Copper is harmless, and is already very common in our daily life. In addition, the cost of copper oxide is only half of that of nickel oxide.

\*Project supported by the National Natural Science Foundation of China (Grant Nos. 51222210 and 11234013) and the One Hundred Talent Project of the Chinese Academy of Sciences.

<sup>†</sup>Corresponding author. E-mail: [yshu@aphy.iphy.ac.cn](mailto:yshu@aphy.iphy.ac.cn)

## 2. Experiment

$\text{Na}_{0.68}\text{Cu}_{0.34}\text{Mn}_{0.66}\text{O}_2$ ,  $\text{Na}_{0.68}\text{Cu}_{0.34}\text{Mn}_{0.50}\text{Ti}_{0.16}\text{O}_2$ , and  $\text{NaCu}_{0.67}\text{Sb}_{0.33}\text{O}_2$  were synthesized in alumina crucibles by conventional solid-state reaction. The precursor materials used here were anhydrous  $\text{Na}_2\text{CO}_3$ ,  $\text{CuO}$ ,  $\text{MnO}_2$ ,  $\text{TiO}_2$ , and  $\text{Sb}_2\text{O}_3$ . They were ground uniformly in stoichiometric proportion and heated in air at  $900\text{ }^\circ\text{C}$  for 15 h to form a single phase. The crystalline structures were characterized by X-ray diffraction, using a Bruker D8 Advance Diffractometer in a transition mode using  $\text{Cu K}\alpha$  radiation. The morphologies of the materials were investigated by a scanning electron microscope (Hitachi S-4800).

The working electrodes were fabricated by spreading the slurry of the active materials (80 wt.%), acetylene black (10 wt.%), and the polyvinylidene fluoride (PVdF, 10 wt.%) on Al foil. The working electrodes were dried at  $120\text{ }^\circ\text{C}$  under vacuum for 10 h to remove the solvent and absorbed water. The coin cells were assembled with sodium metal as counter electrode, 1 M  $\text{NaPF}_6$  in PC as electrolyte, and glass fiber as separator in an argon-filled glove box. The charge and discharge measurements were carried out on a Land BT2000 battery test system (Wuhan, China). Cyclic voltammetry (CV) was measured using Autolab PGSTAT302N (Metrohm, Switzerland).

## 3. Results and discussion

The XRD patterns of the resulting materials are shown in Fig. 1.  $\text{Na}_{0.68}\text{Cu}_{0.34}\text{Mn}_{0.66}\text{O}_2$ , and  $\text{Na}_{0.68}\text{Cu}_{0.34}\text{Mn}_{0.50}\text{Ti}_{0.16}\text{O}_2$  were crystallized in P2 phase, very similar to  $\text{Na}_{0.7}\text{MnO}_2$ <sup>[31]</sup> (S.G.  $P63/mmc$ ), except for a slight  $\text{CuO}$  impurity. However,  $\text{NaCu}_{0.67}\text{Sb}_{0.33}\text{O}_2$  was crystallized in a pure O'3 phase. All the diffraction peaks can be indexed to a monoclinic lattice with space group of  $C2/m$ . In this compound, the  $\text{SbO}_6$  octahedron is surrounded by six  $\text{CuO}_6$  edge-sharing octahedra forming the honeycomb lattice.<sup>[33]</sup> The SEM images in Fig. 2 show that the crystallites of these compounds are highly agglomerated. The particle size of  $\text{Na}_{0.68}\text{Cu}_{0.34}\text{Mn}_{0.66}\text{O}_2$  and  $\text{Na}_{0.68}\text{Cu}_{0.34}\text{Mn}_{0.50}\text{Ti}_{0.16}\text{O}_2$  samples is about 10–20 micrometers, while the particle size is smaller for the  $\text{NaCu}_{0.67}\text{Sb}_{0.33}\text{O}_2$  sample.

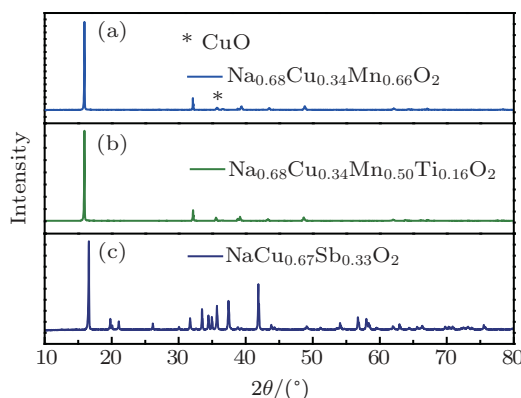


**Fig. 1.** (color online) XRD patterns of the as-prepared (a)  $\text{Na}_{0.68}\text{Cu}_{0.34}\text{Mn}_{0.66}\text{O}_2$ , (b)  $\text{Na}_{0.68}\text{Cu}_{0.34}\text{Mn}_{0.50}\text{Ti}_{0.16}\text{O}_2$ , and (c)  $\text{NaCu}_{0.67}\text{Sb}_{0.33}\text{O}_2$  samples.

The electrochemical behavior of the layered  $\text{Na}_{0.68}\text{Cu}_{0.34}\text{Mn}_{0.66}\text{O}_2$  electrode in sodium-ion batteries was tested by cyclic voltammogram (CV) and galvanostatic charge/discharge cycling. Figure 3(a) shows the cyclic voltammogram curves of the  $\text{Na}_{0.68}\text{Cu}_{0.34}\text{Mn}_{0.66}\text{O}_2$  electrode vs. Na metal between 2.0–4.3 V. A pair of oxidation/reduction peaks is located at 4.1 V and 3.9 V, which corresponds to the redox couple of  $\text{Cu}^{3+}/\text{Cu}^{2+}$ . The difference between them is very small, indicating a small polarization and good kinetics. When discharged to a lower potential, there are two additional pairs of peaks between 2.8–2.2 V. Generally, the reduction potential of tetravalent manganese ( $\text{Mn}^{4+}$ ) in layered oxides is located at about 2.5 V, so the two pairs of peaks might be related to  $\text{Mn}^{4+}/\text{Mn}^{3+}$  redox couple. Figure 3(b) shows the first charge and discharge profiles of  $\text{Na}_{0.68}\text{Cu}_{0.34}\text{Mn}_{0.66}\text{O}_2$  at a current rate of  $C/10$  (note that  $C/10$  refers to 0.34 Na extraction per formula unit in 10 h). The initial charge capacity is 74.5 mAh/g, corresponding to about 0.3 mol Na extraction from  $\text{Na}_{0.68}\text{Cu}_{0.34}\text{Mn}_{0.66}\text{O}_2$ , while  $\text{Cu}^{2+}$  could be oxidized to  $\text{Cu}^{3+}$  at the same time because the valence of Mn here is already 4+. The initial discharge capacity is 67 mAh/g. From the discharge curve, it could be deduced that the capacity above 3.4 V is contributed by the transfer of  $\text{Cu}^{3+}$  to  $\text{Cu}^{2+}$ . As far as we know, this is the highest potential for the redox couple of  $\text{Cu}^{2+}/\text{Cu}^{3+}$ . Below 3.0 V, the capacity is from the reduction of  $\text{Mn}^{4+}$  to  $\text{Mn}^{3+}$ , as discussed above.

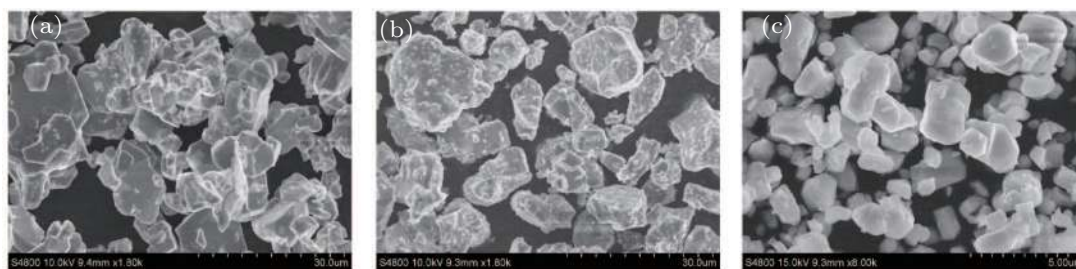


**Fig. 2.** SEM images of (a)  $\text{Na}_{0.68}\text{Cu}_{0.34}\text{Mn}_{0.66}\text{O}_2$ , (b)  $\text{Na}_{0.68}\text{Cu}_{0.34}\text{Mn}_{0.50}\text{Ti}_{0.16}\text{O}_2$ , and (c)  $\text{NaCu}_{0.67}\text{Sb}_{0.33}\text{O}_2$  samples.

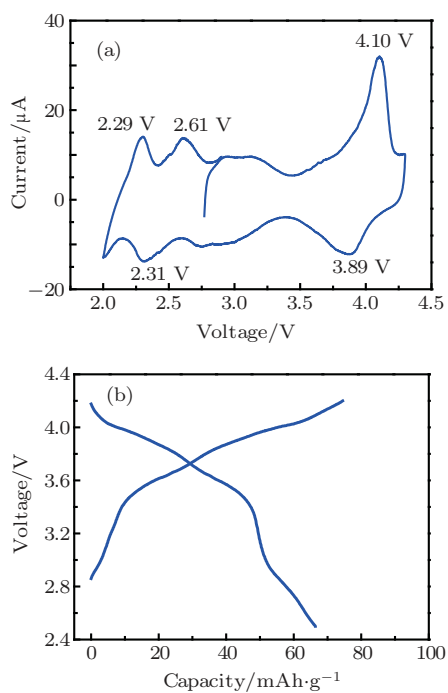


**Fig. 3.** (color online) (a) Cyclic voltammetry (CV) curve and (b) first charge-discharge curves of the  $\text{Na}_{0.68}\text{Cu}_{0.34}\text{Mn}_{0.66}\text{O}_2$  electrode.

We also evaluated the electrochemical performance of the Ti doped compound ( $\text{Na}_{0.68}\text{Cu}_{0.34}\text{Mn}_{0.50}\text{Ti}_{0.16}\text{O}_2$ ) as shown in Fig. 4(a). It can be seen that the charge and discharge curves of the Ti-doped  $\text{Na}_{0.68}\text{Cu}_{0.34}\text{Mn}_{0.66}\text{O}_2$  electrode are much smoother than those of undoped one, showing a more sloping feature which indicates a solid-state reaction rather than a phase transition. This is probably due to a more disordered transition metal arrangement in the transition metal

layer because of the similarity of ionic radii between  $\text{Ti}^{4+}$  and  $\text{Cu}^{2+}$ . However, Ti here may catalyze the decomposition of the electrolyte, because the initial Coulombic efficiency is only 70.6%, much lower than that of the undoped  $\text{Na}_{0.68}\text{Cu}_{0.34}\text{Mn}_{0.66}\text{O}_2$  electrode (89.1%). The second-cycle differential capacity curves of the  $\text{Na}_{0.68}\text{Cu}_{0.34}\text{Mn}_{0.50}\text{Ti}_{0.16}\text{O}_2$  electrode are displayed in Fig. 4(b). They contain two pairs of oxidation/reduction peaks between 3.4–4.1 V. The first pair is located at 3.64 V/3.54 V, while the other pair is located at 3.91 V/4.02 V. The peak difference between each of them is about 0.1 V, very small, indicating a small polarization.

In contrast, the O'3-type  $\text{NaCu}_{0.67}\text{Sb}_{0.33}\text{O}_2$  electrode presents different electrochemical behavior as shown in Fig. 4(c). It can be seen that the electrode can be charged to 4.2 V with a capacity of 90 mAh/g. Three plateaus at 3.6 V, 3.9 V, and 4.1 V in the charge curve can be observed. However, in the discharge process, there is only a small discharge plateau at 4.1 V and the discharge capacity as low as 30 mAh/g, indicating this reaction is almost irreversible. Figure 4(d) displays the first-cycle differential capacity curves of the  $\text{NaCu}_{0.67}\text{Sb}_{0.33}\text{O}_2$  electrode. During the charge, there are three oxidation peaks located at 3.63 V, 3.96 V, and 4.10 V, respectively. However, there is only one reduction peak, located at 4.06 V, related to the fact that the oxidation peak at 4.10 V is reversible. The difference between this pair of peaks is only 0.04 V, showing a much smaller polarization and good kinetics. The reaction mechanism is not clear at the moment, and might be related to the peculiar structure change involved with the interaction of copper and antimony.

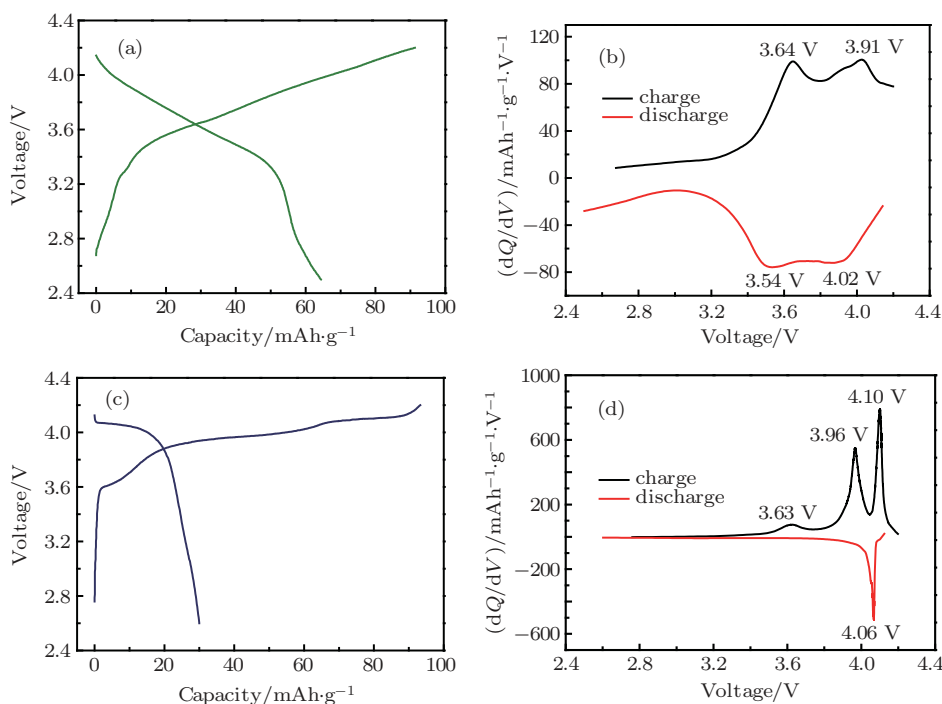


**Fig. 4.** (color online) (a) First charge-discharge curves of the  $\text{Na}_{0.68}\text{Cu}_{0.34}\text{Mn}_{0.50}\text{Ti}_{0.16}\text{O}_2$  electrode; (b) second-cycle differential capacity curves of the  $\text{Na}_{0.68}\text{Cu}_{0.34}\text{Mn}_{0.50}\text{Ti}_{0.16}\text{O}_2$  electrode; (c) first charge-discharge curves of the  $\text{NaCu}_{0.67}\text{Sb}_{0.33}\text{O}_2$  electrode; (d) first-cycle differential capacity curves of the  $\text{NaCu}_{0.67}\text{Sb}_{0.33}\text{O}_2$  electrode.

## 4. Conclusion

In this preliminary study, we synthesized three copper-based layered electrode materials: P2-type  $\text{Na}_{0.68}\text{Cu}_{0.34}\text{Mn}_{0.66}\text{O}_2$ , P2-type  $\text{Na}_{0.68}\text{Cu}_{0.34}\text{Mn}_{0.55}\text{Ti}_{0.16}\text{O}_2$ , and O'3-type  $\text{NaCu}_{0.67}\text{Sb}_{0.33}\text{O}_2$  through simple solid-state method. They are all electrochemically active in sodium-ion batteries. This is the first report of the highly reversible transfer between  $\text{Cu}^{2+}$  and  $\text{Cu}^{3+}$  with high storage potential in secondary batteries. Although the storage capacity is low at moment, we believe that it can be further improved after optimization. The storage mechanism and difference between P2 and O3 layered oxides will be clarified in detail in the near future.

## References

- [1] Armand M and Tarascon J M 2008 *Nature* **451** 652
- [2] Tarascon J M 2010 *Nat. Chem.* **2** 510
- [3] Tarascon J M and Armand M 2001 *Nature* **414** 359
- [4] Pan H, Hu Y S and Chen L 2013 *Energy Environ. Sci.* **6** 2338
- [5] Slater M D, Kim D, Lee E and Johnson C S 2013 *Adv. Funct. Mater.* **23** 947
- [6] Kim S W, Seo D H, Ma X, Ceder G and Kang K 2012 *Adv. Energy Mater.* **2** 710
- [7] Palomares V, Serras P, Villaluenga I, Hueso K B, Carretero-González J and Rojo T 2012 *Energy Environ. Sci.* **5** 5884
- [8] Delmas C, Braconnier J J, Fouassier C and Hagenmuller P 1981 *Solid State Ion.* **3-4** 165
- [9] Mendiboure A, Delmas C and Hagenmuller P 1985 *J. Solid State Chem.* **57** 323
- [10] Doeff M M, Peng M Y, Ma Y and Jonghe L C D 1994 *J. Electrochem. Soc.* **141** L145
- [11] Stevens D A and Dahn J R 2000 *J. Electrochem. Soc.* **147** 1271
- [12] Zhao L, Zhao J, Hu Y S, Li H, Zhou Z, Armand M and Chen L 2012 *Adv. Energy Mater.* **2** 962
- [13] Zhao L, Pan H L, Hu Y S, Li H and Chen L Q 2012 *Chin. Phys. B* **21** 028201
- [14] Sun Y, Zhao L, Pan H, Lu X, Gu L, Hu Y S, Li H, Armand M, Ikuhara Y, Chen L and Huang X 2013 *Nat. Commun.* **4** 1870
- [15] Yu X, Pan H, Wan W, Ma C, Bai J, Meng Q, Ehrlich S N, Hu Y S and Yang X Q 2013 *Nano Lett.* **13** 4721
- [16] Yabuuchi N, Yano M, Yoshida H, Kuze S and Komaba S 2013 *J. Electrochem. Soc.* **160** A3131
- [17] Pan H, Lu X, Yu X, Hu Y S, Li H, Yang X Q and Chen L 2013 *Adv. Energy Mater.* **3** 1186
- [18] Jian Z, Zhao L, Pan H, Hu Y S, Li H, Chen W and Chen L 2012 *Electrochem. Commun.* **14** 86
- [19] Jian Z, Han W, Lu X, Yang H, Hu Y S, Zhou J, Zhou Z, Li J, Chen W, Chen D and Chen L 2013 *Adv. Energy Mater.* **3** 156
- [20] Wang Y, Yu X Q, Xu S Y, Bai J, Xiao R J, Hu Y S, Li H, Yang X Q, Chen L Q and Huang X J 2013 *Nat. Commun.* **4** 2365
- [21] Barpanda P, Oyama G, Nishimura S, Chung S C and Yamada A 2014 *Nat. Commun.* **5** 4358
- [22] Okada S, Takahashi Y, Kiyabu T, Doi T, Yamaki J and Nishida T 2006 210th *ECS Meeting Abstracts*, MA2006-02, 201
- [23] Yabuuchi N, Kajiyama M, Iwatate J, Nishikawa H, Hitomi S, Okuyama R, Usui R, Yamada Y and Komaba S 2012 *Nat. Mater.* **11**
- [24] Sathiyam, Hemalatha K, Ramesha K, Tarascon J M and Prakash A S 2012 *Chem. Mater.* **24** 1846
- [25] Braconnier J J, Delmas C and Hagenmuller P 1982 *Mater. Res. Bull.* **17** 993
- [26] Kim D, Lee E, Slater M, Lu W, Rood S and Johnson C S 2012 *Electrochem. Commun.* **18** 66
- [27] Xu J, Lee D H, Clément R J, Yu X, Leskes M, Andrew, Pell J, Pintacuda G, Yang X Q, Grey C P and Meng Y S 2014 *Chem. Mater.* **26** 1260
- [28] Yabuuchi N, Hara R, Kajiyama M, Kubota K, Ishigaki T, Hoshikawa A and Komaba S 2014 *Adv. Energy Mater.* na
- [29] Kim D, Kang S H, Slater M, Rood S, Vaughey J T, Karan N, Balasubramanian M and Johnson C S 2011 *Adv. Energy Mater.* **1** 333
- [30] Lu Z and Dahn J R 2001 *J. Electrochem. Soc.* **148** A1225
- [31] Delmas C, Fouassier C and Hagenmuller P 1980 *Physica B* **99** 81
- [32] Wang X, Tamaru M, Okubo M and Yamada A 2013 *J. Phys. Chem. C* **117** 15545
- [33] Smirnova O A, Nalbandyan V B, Petrenko A A and Avdeev M 2005 *J. Solid State Chem.* **178** 1165